

Bo Song · Daniel Casem · Jamie Kimberley *Editors*

# Dynamic Behavior of Materials, Volume 1

Proceedings of the 2014 Annual Conference on Experimental  
and Applied Mechanics



Bo Song • Daniel Casem • Jamie Kimberley  
Editors

# Dynamic Behavior of Materials, Volume 1

Proceedings of the 2014 Annual Conference on Experimental  
and Applied Mechanics

*Editors*

Bo Song  
Sandia National Laboratories  
Livermore, CA, USA

Daniel Casem  
U.S. Army Research Laboratory  
Aberdeen Proving Ground, MD, USA

Jamie Kimberley  
New Mexico Institute of Mining  
and Technology  
Socorro, NM, USA

ISSN 2191-5644  
ISBN 978-3-319-06994-4  
DOI 10.1007/978-3-319-06995-1  
Springer Cham Heidelberg New York Dordrecht London

ISSN 2191-5652 (electronic)  
ISBN 978-3-319-06995-1 (eBook)

Library of Congress Control Number: 2014945122

© The Society for Experimental Mechanics, Inc. 2015

This work is subject to copyright. All rights are reserved by the Publisher, whether the whole or part of the material is concerned, specifically the rights of translation, reprinting, reuse of illustrations, recitation, broadcasting, reproduction on microfilms or in any other physical way, and transmission or information storage and retrieval, electronic adaptation, computer software, or by similar or dissimilar methodology now known or hereafter developed. Exempted from this legal reservation are brief excerpts in connection with reviews or scholarly analysis or material supplied specifically for the purpose of being entered and executed on a computer system, for exclusive use by the purchaser of the work. Duplication of this publication or parts thereof is permitted only under the provisions of the Copyright Law of the Publisher's location, in its current version, and permission for use must always be obtained from Springer. Permissions for use may be obtained through RightsLink at the Copyright Clearance Center. Violations are liable to prosecution under the respective Copyright Law.

The use of general descriptive names, registered names, trademarks, service marks, etc. in this publication does not imply, even in the absence of a specific statement, that such names are exempt from the relevant protective laws and regulations and therefore free for general use.

While the advice and information in this book are believed to be true and accurate at the date of publication, neither the authors nor the editors nor the publisher can accept any legal responsibility for any errors or omissions that may be made. The publisher makes no warranty, express or implied, with respect to the material contained herein.

Printed on acid-free paper

Springer is part of Springer Science+Business Media ([www.springer.com](http://www.springer.com))

# Conference Proceedings of the Society for Experimental Mechanics Series

*Series Editor*

Tom Proulx

Society for Experimental Mechanics, Inc.

Bethel, CT, USA

For further volumes:

<http://www.springer.com/series/8922>

## Preface

*Dynamic Behavior of Materials, Volume 1: Proceedings of the 2014 Annual Conference on Experimental and Applied Mechanics* represents one of the eight volumes of technical papers presented at the 2014 SEM Annual Conference & Exposition on Experimental and Applied Mechanics, organized by the Society for Experimental Mechanics and held in Greenville, SC, June 2–5, 2014. The complete proceedings also includes volumes on: *Challenges In Mechanics of Time-Dependent Materials; Advancement of Optical Methods in Experimental Mechanics; Mechanics of Biological Systems and Materials; MEMS and Nanotechnology; Composite, Hybrid, and Multifunctional Materials; Fracture, Fatigue, Failure and Damage Evolution; and Experimental and Applied Mechanics*.

Each collection presents early findings from experimental and computational investigations on an important area within Experimental Mechanics Dynamic Behavior of Materials being one of these areas.

The Dynamic Behavior of Materials track was initiated in 2005 and reflects our efforts to bring together researchers interested in the dynamic behavior of materials and structures and provide a forum to facilitate technical interaction and exchange. In the past years, this track has represented an ever growing area of broad interest to the SEM community, as evidenced by the increased number of papers and attendance.

The contributed papers span numerous technical divisions within SEM, which may be of interest not only to the dynamic behavior of materials community but also to the traditional mechanics of materials community.

The track organizers thank the authors, presenters, organizers, and session chairs for their participation, support, and contribution to this track. We are grateful to the SEM TD chairs who co-sponsor and/or co-organize the sessions in this track. They would also like to acknowledge the SEM support staff for their devoted efforts in accommodating the large number of paper submissions this year, making the 2014 Dynamic Behavior of Materials Track successful.

Livermore, CA, USA  
Aberdeen Proving Ground, MD, USA  
Socorro, NM, USA

Bo Song  
Daniel Casem  
Jamie Kimberley

# Contents

<b>1</b>	<b>Tensile Properties of Dyneema SK76 Single Fibers at Multiple Loading Rates Using a Direct Gripping Method</b>	<b>1</b>
	B. Sanborn and T. Weerasooriya	
<b>2</b>	<b>Statistical Characterization of Single PPTA Fiber Tensile Properties from High Strain Rate Tests</b>	<b>5</b>
	J.H. Kim, N.A. Heckert, W.G. McDonough, K.D. Rice, and G.A. Holmes	
<b>3</b>	<b>Static and Dynamic Thermo-Mechanical Behavior of Ti<sub>2</sub>AlC MAX Phase and Fiber Reinforced Ti<sub>2</sub>AlC Composites</b>	<b>9</b>
	Prathmesh Naik Parrikar, Huili Gao, Miladin Radovic, and Arun Shukla	
<b>4</b>	<b>Effects of Spherical Nanoparticle Addition on Dynamic Properties of Polyamide 11</b>	<b>15</b>
	Masahiro Nishida, Rie Natsume, Norio Fukuda, and Hiroaki Ito	
<b>5</b>	<b>Latest Results in Novel Inertial High Strain Rate Tests</b>	<b>21</b>
	H. Zhu, F. Pierron, and C. Siviour	
<b>6</b>	<b>DIC in Dynamic Punch Testing</b>	<b>27</b>
	J.T. Hammer, T.J. Liutkus, J.D. Seidt, and A. Gilat	
<b>7</b>	<b>Specimen Design to Study the Dynamic Response of an Amorphous Polymer</b>	<b>35</b>
	Mark Foster, Robert Kaste, and Bryan Love	
<b>8</b>	<b>Micro-Raman Spectroscopic Evaluation of Residual Microstresses in Reaction Bonded Boron Carbide Ceramics</b>	<b>39</b>
	Phillip Jannotti and Ghatu Subhash	
<b>9</b>	<b>Dynamic Response of Human Wisdom Teeth and Temporary Fillers</b>	<b>45</b>
	J. Ren, S.H. Wang, C.C. Chiang, and L. Tsai	
<b>10</b>	<b>In Situ and Postmortem Measures of Damage in Polymers at High Strain-Rates</b>	<b>53</b>
	E.N. Brown, K.J. Ramos, D.M. Dattelbaum, B.J. Jensen, A.J. Iverson, C.A. Carlson, K. Fezzaa, G.T. Gray III, B.M. Patterson, C.P. Trujillo, D.T. Martinez, T.H. Pierce, and J. Furmanski	
<b>11</b>	<b>Application of High Speed Imaging in Particle Dynamics Study with Explosives</b>	<b>61</b>
	Elena Jacobs and Vilem Petr	
<b>12</b>	<b>Damage Assessment in Metal Plates by Using Laser Vibrometer Measurements</b>	<b>67</b>
	Zhenhua Tian and Lingyu Yu	
<b>13</b>	<b>Uncertainty of Strain Gage Measurements on Kolsky Bars</b>	<b>73</b>
	Richard L. Rhorer	
<b>14</b>	<b>Full-Field Deformation Observation of Polymer Foam Subjected to Shock Loading</b>	<b>83</b>
	Silas Mallon, Addis Kidane, and Wei-Yang Lu	

<b>15 Explosive Blast Loading of Biosimulants Through Ballistic Protective Materials . . . . .</b>	<b>91</b>
Patrick J. Gillich and Rachel Z. Ehlers	
<b>16 The Hugoniot Relationships for Nonlinear Elastic Substances . . . . .</b>	<b>99</b>
Michael Grinfeld and Pavel Grinfeld	
<b>17 Blast Performance of Foam Filled Sandwich Panels Under Extreme Temperatures . . . . .</b>	<b>107</b>
Payam Fahr, Murat Yazici, and Arun Shukla	
<b>18 Dynamics and Shock Waves in Media with Second Order Phase Transformations . . . . .</b>	<b>113</b>
Pavel Grinfeld and Michael Grinfeld	
<b>19 Structural Changes in Lipid Vesicles Generated by the Shock Waves: Dissipative Particle Dynamics Simulation . . . . .</b>	<b>121</b>
Yelena R. Sliozberg and Tanya L. Chantawansri	
<b>20 Effect of Threaded Joint Preparation on Impact Energy Dissipation Using Frequency-Based Kolsky Bar Analysis . . . . .</b>	<b>127</b>
Brian T. Werner, Bo Song, and Kevin Nelson	
<b>21 Experimental Observation of Slip Pulses During Onset of Sliding Friction . . . . .</b>	<b>133</b>
Vijay Subramanian and Raman P. Singh	
<b>22 Observation of Dynamic Deformation Behavior Around Interface of Bi-material Using DIC . . . . .</b>	<b>141</b>
Yu Oishi, Shuichi Arikawa, Satoru Yoneyama, Hiroyuki Yamada, and Nagahisa Ogasawara	
<b>23 Experimental and Analytical Investigation of Carbon Fiber Cable Damping . . . . .</b>	<b>149</b>
A.K. Maji and Y. Qiu	
<b>24 Volume Damageability According to Criteria of Mechanical and Rolling Fatigue . . . . .</b>	<b>155</b>
Sergei Sherbakov	
<b>25 Developments in the Characterization of Metallic Adhesion . . . . .</b>	<b>161</b>
D. Bortoluzzi, C. Zanoni, J.W. Conklin, and S. Vitale	
<b>26 Stress Initiation and Propagation in Glass During Ring-on-Ring Testing . . . . .</b>	<b>167</b>
Costas G. Fountzoulas, Jeffrey J. Swab, and Parimal J. Patel	
<b>27 Investigation of Cavitation Using a Modified Hopkinson Apparatus . . . . .</b>	<b>177</b>
Dilaver Singh and Duane S. Cronin	
<b>28 Characterization of Structural Epoxy Adhesives . . . . .</b>	<b>185</b>
Luis F. Trimiño, Duane S. Cronin, and Mary M. Caruso Dailey	
<b>29 Rate Dependent Response of Cross-Linked Epoxy Networks . . . . .</b>	<b>193</b>
Randy A. Mrozek, Mark Hindenlang, Adam Richardson, Kevin A. Masser, Jian H. Yu, and Joseph L. Lenhart	
<b>30 Dynamic Crack Propagation in Layered Transparent Materials Studied Using Digital Gradient Sensing Method . . . . .</b>	<b>197</b>
Balamurugan M. Sundaram and Hareesh V. Tippur	
<b>31 Fracture Toughness Testing of Advanced Silicon Carbide Ceramics Using Digital Image Correlation . . . . .</b>	<b>207</b>
John Pittari III and Ghatu Subhash	
<b>32 Fracture of Pre-stressed Woven Glass Fiber Composite Exposed to Shock Loading . . . . .</b>	<b>213</b>
Silas Mallon, Behrad Koohbor, and Addis Kidane	
<b>33 A Miniature Tensile Kolsky Bar for Thin Film Testing . . . . .</b>	<b>221</b>
Jamie Kimberley and Justin Paul	
<b>34 High Temperature Tension HSB Device Based on Direct Electrical Heating . . . . .</b>	<b>227</b>
M. Hokka, K. Östman, J. Rämö, and V.-T. Kuokkala	

<b>35</b>	<b>Dynamic Flow Stress Measurements for Machining Applications . . . . .</b>	<b>235</b>
	Steven Mates, Eran Vax, Richard Rhorer, Michael Kennedy, Eric Whintenton, Stephen Banovic, and Tim Burns	
<b>36</b>	<b>Thermo-Mechanical Behavior of AA-2219 and AA-2195 at High Strain Rates . . . . .</b>	<b>241</b>
	Vinod Pare and Krishna N. Jonnalagadda	
<b>37</b>	<b>Rigid Angular Impact Responses of a Generic Steel Vehicle Front Bumper and Crush Can: Correlation of Two Velocity-Measurement Techniques . . . . .</b>	<b>249</b>
	A. Seyed Yaghoubi, P. Begeman, G. Newaz, D. Board, Y. Chen, and O. Faruque	
<b>38</b>	<b>Force-Time History Assessment of a Generic Steel Vehicle Front Bumper and Crush Can Subjected to a Rigid Center Pole Impact . . . . .</b>	<b>257</b>
	A. Seyed Yaghoubi, P. Begeman, G. Newaz, D. Board, Y. Chen, and O. Faruque	
<b>39</b>	<b>Damage of Two Concrete Materials due to Enhanced Shaped Charges . . . . .</b>	<b>267</b>
	A.D. Resnyansky and S.A. Weckert	
<b>40</b>	<b>Influence of Free Water and Strain-Rate on the Behaviour of Concrete Under High Confining Pressure . . . . .</b>	<b>279</b>
	P. Forquin	
<b>41</b>	<b>Numerical Investigation of Impact Condition Effects on Concrete Penetration . . . . .</b>	<b>285</b>
	Christopher S. Meyer	
<b>42</b>	<b>On the Damage Mechanisms Involved in Different Geomaterials Subjected to Edge-on Impact Experiments . . . . .</b>	<b>295</b>
	P. Forquin	
<b>43</b>	<b>Effect of Boundary Conditions on the Thermo-Mechanical Response of Hastelloy<sup>®</sup> X Plates Subjected to Shock Loading . . . . .</b>	<b>301</b>
	C. Anil Rajesh, P. Naik Parrikar, S. Abotula, and A. Shukla	
<b>44</b>	<b>Experimental Studies of the Matrix Detonating Cord Charge . . . . .</b>	<b>307</b>
	Vilem Petr and Steven Beggs	
<b>45</b>	<b>The Characterization of Ammonium Nitrate Mini-Prills . . . . .</b>	<b>319</b>
	Erica Lotspeich and Vilem Petr	
<b>46</b>	<b>High-Strain Rate Compressive Behavior of Dry Mason Sand Under Confinement . . . . .</b>	<b>325</b>
	Huiyang Luo, Yingjie Du, Zhenxing Hu, and Hongbing Lu	
<b>47</b>	<b>Scale Bridging Interactions During Penetration of Granular Materials . . . . .</b>	<b>335</b>
	M. Omdivar, Z. Chen, S. Bless, and M. Iskander	
<b>48</b>	<b>Experimental Investigation on Material Dynamic Behaviors Using Ultra-high-speed Cameras . . . . .</b>	<b>341</b>
	Xing Zhao, Silas Mallon, Addis Kidane, Michael Sutton, and Hubert Schreier	
<b>49</b>	<b>Application of 3-D Digital Image Correlation Technique to Study Underwater Implosion . . . . .</b>	<b>351</b>
	Sachin Gupta, Venkitanarayanan Parameswaran, Michael Sutton, and Arun Shukla	
<b>50</b>	<b>Dynamic Analysis of a Plate Loaded by Explosively Driven Sand . . . . .</b>	<b>357</b>
	A.D. Resnyansky and S.A. Weckert	
<b>51</b>	<b>Simulating the Planar Shock Response of Concrete . . . . .</b>	<b>369</b>
	Jeff LaJeunesse, John Borg, and Brad Martin	
<b>52</b>	<b>Mesoscale Simulations of Dry Sand . . . . .</b>	<b>379</b>
	Merit G. Schumaker, John P. Borg, Gregory Kennedy, and Naresh N. Thadhani	
<b>53</b>	<b>Perforation of 6082-T651 Aluminum Plates with 7.62 mm APM2 Bullets at Normal and Oblique Impacts . . . . .</b>	<b>389</b>
	M.J. Forrestal, T.L. Warren, T. Børvik, and W. Chen	



# Chapter 1

## Tensile Properties of Dyneema SK76 Single Fibers at Multiple Loading Rates Using a Direct Gripping Method

B. Sanborn and T. Weerasooriya

**Abstract** Ultra-high-molecular-weight polyethylene (UHMWPE) fibers such as Dyneema and Spectra are seeing more use in lightweight armor applications due to higher tensile strength and lower density compared with aramid fibers such as Kevlar and Twaron. Numerical modeling is used to design more effective fiber-based composite armor. For accurate simulation of ballistic impacts, material response such as tensile stress-strain of the composite constituents must be studied under experimental conditions similar to ballistic events. UHMWPE fibers are difficult to grip using adhesive methods typically used for other fibers due to low surface energy. Based on previous studies, the ability to grip UHMWPE fibers using traditional adhesive methods depends on fiber diameter and is limited to smaller diameter fibers that could affect reported stress values. To avoid diameter restrictions and surface energy problems, a direct gripping method has been used to characterize Dyneema SK76 single fibers at strain rates of 0.001 s<sup>-1</sup>, 1 s<sup>-1</sup>, and 1000 s<sup>-1</sup>. In this report, the dependence of fiber diameter and gage length on failure strength is discussed as well as success rate of failures in the gage section with this gripping technique. A comparison of the tensile properties with previous studies is also explored.

**Keywords** Single fiber • SHTB • Dyneema • UHMWPE • Tensile response

### 1.1 Introduction

Aramid fibers such as Kevlar and Twaron are frequently used in protective armor, though ultrahigh molecular weight polyethylene (UHMWPE) fibers such as Dyneema and Spectra are desirable due to lower density at 0.97 g/cm<sup>3</sup> compared to 1.44 g/cm<sup>3</sup> for aramids, as well as higher tensile modulus and good resistance to chemical and physical degradation. Due to an increasing need for numerical modeling capability of different soft armor systems, constituent level material properties are required to develop simulation methods. The primary loading mode on fibers used in protective equipment is axial tension. Hence, tensile experiments must be conducted at high strain rates that mimic loading rates that are seen in an impact event. UHMWPE fibers such as Dyneema and Spectra are notoriously difficult to grip for these tensile tests due to low surface energy [1]. Several authors have reported difficulties associated with gripping UHMWPE fibers [2, 3].

The ability to grip Dyneema and other UHMWPE fibers using the standard gripping method for fibers which utilizes an adhesive to attach the fibers to a cardboard substrate is apparently dependent on fiber diameter [4, 5], which can be used successfully when diameter is limited to up to 16  $\mu\text{m}$  as noted by Hudspeth et al. [5]. Hybrid methods utilizing mechanical gripping and adhesives have also shown limited success rates and some authors have indicated that fibers slip in the grips during tensile experiments [2, 3]. Though adhesive methods are effective for aramid fibers [6–10], Kim et al. [11–13] have been developing a method of direct gripping on PPTA. This direct clamping method utilizes poly methyl methacrylate (PMMA) blocks. The efficacy of this method to grip Kevlar fibers has been rigorously studied using a variety of statistical

---

B. Sanborn (✉)

Oak Ridge Institute for Science and Education/US Army Research Laboratory, Bldg 4600,  
Aberdeen Proving Ground, Aberdeen, MD, USA  
e-mail: brett.sanborn2.ctr@mail.mil

T. Weerasooriya

US Army Research Laboratory, Bldg 4600, Aberdeen Proving Ground, Aberdeen, MD, USA

methods at different strain rates, including high strain rates which pose additional problems such as minimizing the overall grip size to fit on the Kolsky bar apparatus [11–13].

To overcome the difficulties associated with adhesive bonding, hybrid adhesive and mechanical methods, and mechanical methods that might not provide accurate strain measurements, a gripping method similar to that proposed by Kim et al. [11–13] has been refined and used in this study to collect accurate strain histories of single fiber samples and to load specimens to failure without apparent fiber slippage from the gripping system. Furthermore, this technique is applicable to UHMWPE fibers and is not limited by the diameter of the fiber and can be utilized at high strain rates. In addition to investigating the loading rate effects on SK76 fibers, a wide range of gage lengths was used to study the effect of defect distribution in the fiber.

## 1.2 Experiments

To study the tensile strength of Dyneema SK76 fiber under uniaxial tension, single fibers were extracted from SK76 yarns and were glued to temporary specimen holders. Diameters of individual fiber samples were measured in an optical microscope for accurate stress determination. After diameter measurements were taken, the fibers were loaded into the direct grips and clamped in place. The temporary specimen holders were clipped and removed from the experimental apparatus. Fiber samples were pulled in tension at strain rates of 0.001 and 1 s<sup>-1</sup> using Bose Electroforce and at 1,000 s<sup>-1</sup> using a tension Kolsky bar modified for fiber characterization. Specimens with gage lengths of 5, 10, and 50 mm were studied at quasi-static and intermediate rates and gage lengths of 5, 7, and 10 mm were studied at high strain rates to study the effect of defect distribution in the fibers. A total of ten experiments were conducted at each condition of gage length and strain rate for a total of 90 experiments.

## 1.3 Results

Overall, the direct gripping method applied to Dyneema fibers was successful. Fibers over a range of from 14.5 to 22.3 μm were successfully gripped using this technique. One particularly large fiber sample with diameter of 35.9 ± 0.52 μm was also successfully gripped using this technique, but was not included in the analysis due to its uncharacteristically large diameter.

Tensile strength as a function of strain rate is shown in Fig. 1.1. The overall behavior of the fiber shows an increase in strength with increasing strain rate. The results show that a plateau in strength is reached at an intermediate strain rate of 1 s<sup>-1</sup> since the failure strength of the fiber does not increase when the strain rate is increased from 1 to 1,000 s<sup>-1</sup>. The

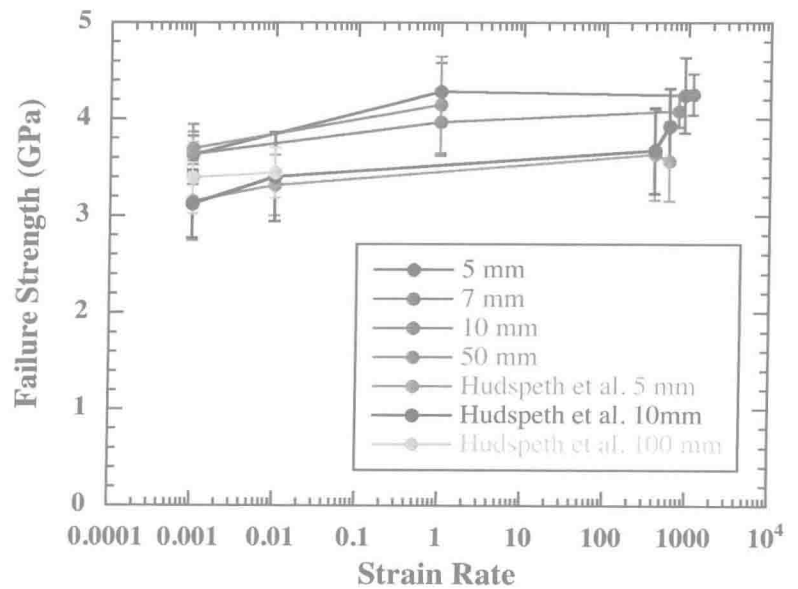
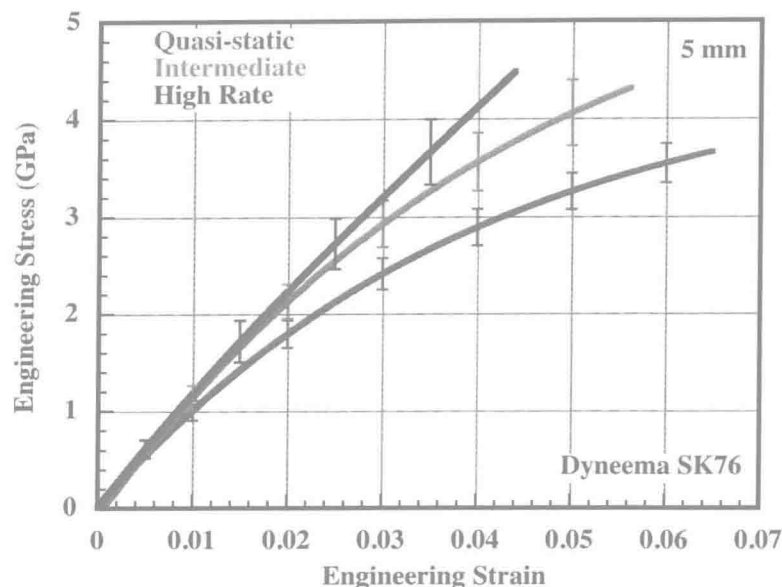


Fig. 1.1 Tensile strength as a function of strain rate

**Fig. 1.2** Stress–strain response at multiple strain rates. Note the increase in linearity for the same gage length with increasing strain rate. The curves in these plots represent the average behavior of ten experiments



failure strength of Dyneema does not depend on the gage length of the fiber since no change in strength was observed at shorter gage lengths. Future work should include shorter gage lengths to further probe this observation. The results of this study show higher failure strengths compared to the study by Hudspeth et al. [5] on Dyneema SK76, but compare well with published data by Dyneema [14] and a study by Russell et al. on SK76 fibers and yarns [3].

In general, the stress–strain behavior of the Dyneema fiber is increasingly linear with increasing strain rate [3, 15, 16]. The average behavior of 5 mm gage length samples is shown in Fig. 1.2. Error bars represent  $\pm$  one standard deviation of strength at each strain value. At low rates, the primary deformation mode of the Dyneema UHMWPE fiber is creep [3, 17–19]. Creep was also noted on non-ballistic grades of Dyneema such as SK66 [20] and SK65 [21]. In each case the creep component increases with decreasing strain rate. The increase in linearity of the stress–strain curve is also seen when experiments at different temperatures are conducted [20] suggesting that the mechanism of failure at low temperatures is similar the mechanism of failure at high strain rates.

## References

1. Lin SP, Han JL, Yeh JT, Chang FC, Hsieh KH (2007) Surface modification and physical properties of various UHMWPE fiber reinforced modified epoxy composites. *J Appl Polym Sci* 104:655–665
2. Umberger PD (2010) Characterization and response of thermoplastic composites and constituents. Master's thesis
3. Russell BP, Karthikeyan K, Deshpande VS, Fleck NA (2013) The high strain rate response of ultra high molecular weight polyethylene: from fibre to laminate. *Int J Impact Eng* 60:1–9
4. Cochran S, Galvez F, Pintor A, Cendon D, Rosello C, Sanchez-Galvez V (2002) Characterization of fraglight non-woven felt and simulation of FSP's impact in it. R&D 8927-AN-01
5. Hudspeth M, Nie X, Chen W (2012) Dynamic failure of Dyneema SK76 single fibers under biaxial shear/tension. *Polymer* 53:5568–5574
6. Lim J, Zheng JQ, Masters K, Chen WW (2010) Mechanical behavior of A265 single fibers. *J Mater Sci* 45:652–661
7. Lim J, Chen WW, Zheng JQ (2010) Dynamic small strain measurements of Kevlar® 129 single fibers with a miniaturized tension Kolsky bar. *Polym Test* 29:701–705
8. Lim J, Zheng JQ, Masters K, Chen WW (2011) Effects of gage length loading rates, and damage on the strength of PPTA fibers. *Int J Impact Eng* 38:219–227
9. Cheng M, Chen W, Weerasooriya T (2005) Mechanical properties of Kevlar KM2 Single fiber. *J Eng Mater Technol* 127:197–203
10. Sanborn B, Weerasooriya T (2013) Quantifying damage at multiple loading rates to Kevlar KM2 fibers due to weaving and finishing. ARL-TR-6465. June 2013
11. Kim JH, Heckert AN, Leigh SD, Rhorer RL, Kobayashi H, McDonough WG, Rice KD, Holmes GA (2014) Statistical analysis of PPTA fiber strengths measured under high strain rate condition. *Compos Sci Technol* 98:93–99
12. Kim JH, Heckert NA, McDonough WG, Rice KD, Holmes GA (2013) Single fiber tensile properties measured by the Kolsky bar using a direct fiber clamping method. In: *Proceedings of society for experimental mechanics conference*. Lombard, IL
13. Kim JH, Heckert NA, Leigh SD, Kobayashi H, McDonough WG, Rice KD, Holmes GA (2013) Effects of fiber gripping methods on the single fiber tensile test: I. Non-parametric statistical analysis. *J Mater Sci* 48:3623–3673

14. Dyneema Comprehensive Fact Sheet (2008) January 2008. REF: CIS YA100
15. Cansfield D, Ward I, Woods D, Buckley A, Pierce J, Wesley J (1983) Tensile strength of ultra high modulus linear polyethylene filaments. *Polym Commun* 24:130e1
16. Schwartz P, Netravali A, Sembach S (1986) Effects of strain rate and gauge length on the failure of ultrahigh strength polyethylene. *Text Res J* 56(8):502–508
17. Wilding MA, Ward IM (1978) Tensile creep and recovery in ultra-high modulus linear polyethylenes. *Polymer* 19:969–976
18. Wilding MA, Ward IM (1978) Creep and recovery in ultra-high modulus polyethylene. *Polymer* 22:870–876
19. Wilding MA, Ward IM (1984) Creep and Stress-relaxation in ultra-high modulus linear polyethylene. *J Mater Sci* 19:629–636
20. Govaert LE, Bastiaansen CWM, Leblans PJR (1993) Stress–strain analysis of oriented polyethylene. *Polymer* 34(3):534–540
21. Liu X, Yu W (2005) Evaluation of the tensile properties and thermal stability of ultrahigh-molecular-weight polyethylene fibers. *J Appl Polym Sci* 97:310–315

## Chapter 2

# Statistical Characterization of Single PPTA Fiber Tensile Properties from High Strain Rate Tests

J.H. Kim, N.A. Heckert, W.G. McDonough, K.D. Rice, and G.A. Holmes

**Abstract** Single [poly (*p*-phenylene terephthalamide)] PPTA fiber tensile strengths were measured under quasi-static and high strain rate loading conditions, and poly (methyl methacrylate) (PMMA) and rubber as gripping materials were used to investigate gripping effects for the tests. To incorporate the strength distributions of single PPTA fibers into a rate dependent stochastic strength model, it is important to estimate uncertainties of the model parameters as well as the best-fitting-distribution for the parameter estimation. We demonstrated the appropriateness of a Weibull model for the tensile strengths obtained by the quasi-static test and preliminary results for the corresponding Weibull shape parameters with approximately  $\pm 20\%$  parameter confidence intervals. These results will be used to characterize of the strengths obtained by the high strain rate test using the Weibull model.

**Keywords** Single fiber tensile test • PPTA fiber • Statistical analysis • High strain rate • Direct fiber grip

## 2.1 Introduction

Soft body armors have been used to protect the human body from the ballistic impact. The impact and perforation of fabrics in the body armors depend on several parameters including the material properties of the yarns, fabric structure, the projectile velocity etc. When a projectile strikes a fabric of body armor, longitudinal and transverse waves propagate from the impact zone, and these create fiber deformations in several different directions indicating tension along the fiber's axis, transverse compression, and fiber deflection. Numerous studies have been carried out on the impact behaviors of soft body armors during ballistic events, however, most of the studies on the influence of materials tensile properties on ballistic performance are conducted using the quasi-static properties [1].

Until recently, most fiber strengths obtained by single fiber tensile tests have been performed under many orders of magnitude slower loading conditions compared to ballistic impact. In order to measure fiber strengths under loading rates comparable to those of ballistic impact, a miniaturized Kolsky bar has been developed [2] and a direct fiber gripping method to increase test throughput has been adopted after a comparison study for gripping methods [3, 4].

Fiber strengths obtained by the single fiber tensile test typically exhibit large variation, so statistical analyses are often carried out to model dispersions of strength data. Many Weibull analyses for single fiber strengths obtained under the quasi-static loading conditions have been carried out; however fiber strengths for high strain rates tests are rarely reported.

---

Official contribution of the National Institute of Standards and Technology; not subject to copyright in the United States.

J.H. Kim • W.G. McDonough • G.A. Holmes (✉)

Materials Science and Engineering Division (M/S 8541), National Institute of Standards and Technology,  
Gaithersburg, MD 20899, USA  
e-mail: gale.holmes@nist.gov

N.A. Heckert

Statistical Engineering Division (M/S 8980), National Institute of Standards and Technology,  
Gaithersburg, MD 20899, USA

K.D. Rice

Materials Measurement Science Division (M/S 8102), National Institute of Standards and Technology,  
Gaithersburg, MD 20899, USA

Main objectives of this study are investigating stochastic the behavior of single PPTA fiber strengths obtained under the quasi-static and high rate loading tests. We focus on the Weibull distribution to model the strength dispersions, after examining distributions graphically.

## 2.2 Stochastic Fiber Fracture Model

A stochastic fiber fracture model using the two-parameter Weibull distribution has been proposed to predict ultimate strengths of various types of fibers [5]. The average tensile strength ( $\sigma_f$ ) of the individual fibers with a length ( $L$ ) can be given by:

$$\sigma_f = \gamma \left( \frac{L}{L_0} \right)^{-1/\beta} \Gamma \left( 1 + \frac{1}{\beta} \right), \quad (2.1)$$

where  $\gamma$  and  $\beta$  are the Weibull scale and shape parameters respectively, and  $\Gamma$  is the gamma function.  $\Gamma(1 + 1/\beta) \approx 0.95 \pm 0.03$  in the case of the Weibull shape parameter  $\beta$  values varying from 5 to 30 [5].  $L_0$  is a reference length (1 mm in this study). Equation (2.1) is typically used for estimating fiber strengths obtained by quasi-static tests. Assuming the same linear elastic behaviors of the fibers until rupture for both quasi-static and high strain rate loadings, the relation of the Weibull parameters between quasi-static and high strain rate tests as a function of strain rate can be given by [6]:

$$\begin{cases} \beta_s = \beta_h \\ \gamma_s = \left[ 1 + E \left( \frac{\dot{\epsilon}}{\dot{\epsilon}_{ref}} \right) \right] \left[ 1 + \epsilon \left( \frac{\dot{\epsilon}}{\dot{\epsilon}_{ref}} \right) \right] \gamma_h \end{cases} \quad (2.2)$$

where the subscripts  $s$  and  $h$  represent quasi-static and high strain rate loading conditions, and  $\dot{\epsilon}$  and  $\dot{\epsilon}_{ref}$  represent the input strain rate and the reference strain rate (i.e. the strain rate for quasi-static loading) respectively. The ratio of the mean strengths for the two cases is  $\gamma_s \left( \frac{L}{L_0} \right)^{-1/\beta_s} \Gamma \left( 1 + \frac{1}{\beta_s} \right) / \gamma_h \left( \frac{L}{L_0} \right)^{-1/\beta_h} \Gamma \left( 1 + \frac{1}{\beta_h} \right)$ . So if two cases (i.e., quasi-static and high strain rate) are adequately modelled by the two-parameter Weibull and the shape parameters are essentially equivalent, then the ratio simplifies to the ratio of the scale parameters.

## 2.3 Experimental Procedure

### 2.3.1 Single Fiber Tensile Tests

PMMA [poly (methyl methacrylate)] and rubber were used as clamp materials for the single fiber tensile tests to investigate gripping effects. The authors will utilize the term ‘‘PMMA and rubber grips’’ to refer a fiber grip made by two different materials set. For the quasi-static loading, a single fiber was clamped in the grips of a screw-driven machine with approximately 1 mN of pretension using a weight. Open/close motions of the grips were controlled by a pneumatic controller. Strain-to-failure was obtained by the displacement of the actuator, and the tensile stress was obtained by the force history and the cross sectional area of the fiber. Fiber lengths of 2, 5, and 10 mm were chosen to be the gauge lengths respectively. For the high rate loading, the miniaturized Kolsky bar was used in conjunction with a quartz-piezoelectric load cell due to very small transmitted force signal through a single PPTA fiber. A laser optical system [7] was used to measure the displacement of the Kolsky bar. A thin laser line generated by 100 mW laser illuminates a target that is attached to the gripping area of the Kolsky bar. The intensity of the refocused beam from the laser line is increased as the end of the bar moves in uniaxial tension and the relation between the bar location and the laser intensity is used to calibrate the laser intensity. Fiber lengths with 2, 5, and 8 mm were used as the gauge lengths of the high rate tests. Both tensile test results as a function of strain rate will be demonstrated in the presentation.

## 2.4 Results and Discussion

In this section, the procedures of the statistical analyses for the tensile strength data are briefly described and the statistical analysis results are summarized for each step.

### 2.4.1 Non-parametric Analysis of the Tensile Strengths

The fiber tensile strengths obtained by PMMA and rubber grips were compared graphically using kernel density plots. The kernel density estimate is defined as

$$f(y) = \frac{\sum_{i=1}^n K\left\{\frac{(y - Y_i)}{h}\right\}}{nh}, \quad (2.3)$$

with  $K$ ,  $h$ ,  $Y_i$ , and  $n$  denoting the kernel function, the window width, the  $i$ th data point and the number of data points, respectively. The histogram is a simple kernel density estimator where  $h$  corresponds to the bin width, but typically the kernel density plot can show the underlying structure in the data more clearly than a histogram, particularly for modest sample sizes. Kernel density plots provide indications of such features as (1) the center of the data, (2) the spread of the data, and (3) the skewness of the data. Because of these advantages, we used it for estimating the strength distributions graphically. Figure 2.1 shows the kernel density plots of the tensile strengths for the PMMA and rubber grip tests using 2 mm fibers under the quasi-static loading condition. Similar widths of the kernel density plots for both grip tests indicate comparable strength distributions for the tests, but with possibly distinct modes of peak locations.

### 2.4.2 Distributional Fits: Parameter Estimates and Confidence Limits

Since the parameters of the two-parameter Weibull distribution are used in estimating average fiber strengths, one should estimate the Weibull parameters and uncertainties (confidence intervals) for the parameter estimates. The cumulative distribution function of the two-parameter Weibull distribution is given by:

$$F = 1 - \exp\left(-\frac{L}{L_0}\left(\frac{x}{\gamma}\right)^\beta\right), \quad (2.4)$$

where  $x$  is fiber strength and other parameters are the same with those in Eq. (2.1). Although the Weibull plot is frequently used to estimate the parameters, we used maximum likelihood (ML) method. Since the Weibull shape parameter is

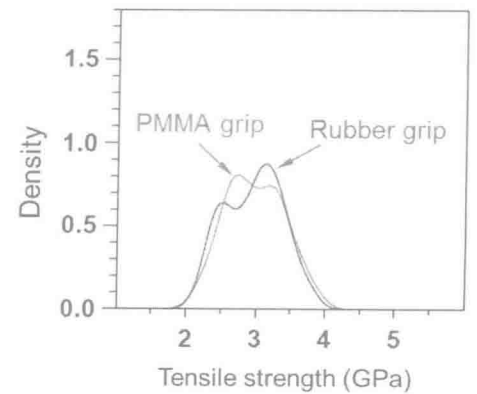


**Fig. 2.1** Kernel density plot for the fiber strengths obtained by PMMA and rubber grips

correlated to the dispersion of the data, we focus on the shape parameter and its confidence interval. The shape parameters for the strength data (Fig. 2.1) obtained by the ML method varied from six to eight with confidence intervals approximately  $\pm 20\%$ .

### 2.4.3 Assessing Goodness of Fit

The two-parameter Weibull distribution is typically used to analyze dispersions of fiber strength data without investigating goodness of fit. A primary analytical method to assess goodness-of-fit is the Anderson–Darling (AD) test. Using PPTA fibers similar to the fibers used in this study, fiber strengths with 2 mm were previously measured for the PMMA grip under the quasi-static loading condition. A–D tests were carried out, which rejected the best-fitting assumption for the two-parameter Weibull distribution (1.2 A–D and 0.76 critical values). More goodness-of-fit analyses are being carried out with the PPTA fibers for the PMMA and rubber grips and will be presented in the future.

## 2.5 Concluding Remarks

Single PPTA fiber strengths were measured using the PMMA and rubber grip methods under quasi-static and high strain rate loading conditions. To validate a model, an important procedure is to confirm the best-fitting distribution as well as the parameter estimates. Since we are investigating dispersions of fiber strengths obtained by the high rate tests which are rarely reported in literatures, a procedure for assessing the strength distributions with the two-parameter Weibull is demonstrated for each step. Detailed statistical investigations for the strengths will be used to characterize PPTA fiber tensile properties as a function of loading rate and gripping method.

## References

1. Cheeseman BA, Bogetti TA (2003) Ballistic impact into fabric and compliant composite laminates. *Compos Struct* 61:161–173
2. Cheng M, Chen W, Weerasooriya T (2004) Mechanical properties of Kevlar KM2 single fiber. *Int J Solids Struct* 41:6215–6232
3. Kim JH, Heckert NA, Leigh SD, Kobayashi H, McDonough WG, Rice KD, Holmes GA (2013) Effects of fiber gripping methods on the single fiber tensile test: I. Non parametric statistical analysis. *J Mater Sci* 48:3623–3637
4. Kim JH, Heckert NA, Leigh SD, Rhorer RL, Kobayashi H, McDonough WG, Rice KD, Holmes GA (2012) Statistical analysis of PPTA fiber strengths measured under high strain rate condition. *Compos Sci Technol* 98(2014):93–99 (10.1016/j.compscitech.2012.03.021)
5. Vanderzwaag S (1989) The concept of filament strength and the weibull modulus. *J Test Eval* 17:292–298
6. Xia YM, Yuan JM, Yang BC (1994) A statistical-model and experimental-study of the strain-rate dependence of the strength of fibers. *Compos Sci Technol* 52:499–504
7. Lim J, Chen WNW, Zheng JQ (2010) Dynamic small strain measurements of Kevlar 129 single fibers with a miniaturized tension Kolsky bar. *Polym Test* 29:701–705



## Chapter 3

# Static and Dynamic Thermo-Mechanical Behavior of $\text{Ti}_2\text{AlC}$ MAX Phase and Fiber Reinforced $\text{Ti}_2\text{AlC}$ Composites

Prathmesh Naik Parrikar, Huili Gao, Miladin Radovic, and Arun Shukla

**Abstract**  $\text{Ti}_2\text{AlC}$  MAX phase samples were processed by using Spark Plasma Sintering from commercially available  $\text{Ti}_2\text{AlC}$  powder. Static and dynamic loading was performed by Universal Testing Machine and Split Hopkinson Pressure Bar (SHPB) respectively. The SHPB apparatus was modified to investigate the dynamic fracture initiation toughness. High speed photography was used to determine the fracture initiation time and the associated failure load. To widen applications, 20 vol % fiber of Nextel<sup>TM</sup>-610 and Nextel<sup>TM</sup>-720 have been added for the reinforcement of  $\text{Ti}_2\text{AlC}$ , respectively. The results reveal that the peak compressive failure stress in dynamic conditions decreases with increasing temperatures, from 1,645 MPa at 25 °C to 1,210 MPa at 1,200 °C. The fracture experiments show that the dynamic fracture toughness is higher than the quasi-static value by approximately 35 %. The fracture toughness decreases with increase in temperature. The post mortem analysis of the fracture surfaces conducted using Scanning Electron Microscopy revealed that kinking along with intergranular cracking and delamination play important role in deformation of  $\text{Ti}_2\text{AlC}$ . Compared to pure  $\text{Ti}_2\text{AlC}$ , compressive fracture strength of 20 vol%  $\text{Ti}_2\text{AlC}/720\text{f}$  and  $\text{Ti}_2\text{AlC}/610\text{f}$  composites were enhanced by 39.7 and 32.6 % under static loading.

**Keywords** MAX phase • Thermo-mechanical loading • Fracture toughness • Constitutive behavior • Kink bands • Titanium aluminum carbide

## 3.1 Introduction

The  $\text{M}_{n+1}\text{AX}_n$  (MAX) phases are a class of nanolayered, machinable, early transition ternary metal carbides and/or nitrides [1]. Because of the structural similarity between MAX phases and their corresponding MX structure, they share lot of properties while some properties are significantly different from their MX counterparts [2, 3].

$\text{Ti}_2\text{AlC}$  is a MAX phase that has attracted a lot of attention as it is machinable, electrically conductive, lightweight and resistant to thermal shock, oxidation and creep [4–7]. Different methods of fabrication of  $\text{Ti}_2\text{AlC}$  and its composites for high temperature applications [4, 8, 9]. The material characterization of MAX phases has been limited to quasi-static loading regimes. The  $K_{\text{I}}$  values are reported to be in a large range from 4 to 16  $\text{MPa m}^{1/2}$  are probably attributed to the different grain size, the shape and dimension of the sample, sample impurities, different testing methods, and experimental conditions [10–13].

In this study experiments were conducted to investigate the effect of different strain rate and temperature on the material characteristics. An experimental investigation of the stress strain characteristics of  $\text{Ti}_2\text{AlC}$  under quasi-static and dynamic loading was conducted at room and elevated temperatures. The peak compressive stress decreases with increasing

---

P. Naik Parrikar • A. Shukla (✉)

Department of Mechanical, Industrial and Systems Engineering, University of Rhode Island, Kingston, RI 02881, USA  
e-mail: shuklaa@egr.uri.edu

H. Gao

Mechanical Engineering Department, Texas A&M University, College Station, TX 77843, USA

M. Radovic

Mechanical Engineering Department, Texas A&M University, College Station, TX 77843, USA

Materials Science and Engineering Department, Texas A&M University, College Station, TX 77843, USA

B. Song et al. (eds.), *Dynamic Behavior of Materials, Volume 1: Proceedings of the 2014 Annual Conference on Experimental and Applied Mechanics*, Conference Proceedings of the Society for Experimental Mechanics Series, DOI 10.1007/978-3-319-06995-1\_3, © The Society for Experimental Mechanics, Inc. 2015

9